DISCLAIMER

This report was prepared as an account of work sponsored by an agency of the United States Government. Neither the United States Government nor any agency thereof, nor any of their employees, makes any warranty, express or implied, or assumes any legal liability or responsibility for the accuracy, completeness, or usefulness of any information, apparatus, product, or process disclosed, or represents that its use would not infringe privately owned rights. Reference herein to any specific commercial product, process, or service by trade name, trademark, manufacturer, or otherwise does not necessarily constitute or imply its endorsement, recommendation, or favoring by the United States Government or any agency thereof. The views and opinions of authors expressed herein do not necessarily state or reflect those of the United States Government or any agency thereof. Reference herein to any social initiative (including but not limited to Diversity, Equity, and Inclusion (DEI); Community Benefits Plans (CBP); Justice 40; etc.) is made by the Author independent of any current requirement by the United States Government and does not constitute or imply endorsement, recommendation, or support by the United States Government or any agency thereof.

ORNL/SPR-2024/3714
CPS 36805

Development of High-Temperature (>700°C) Molten Salt Pump Technology for Generation 3 Solar Power Tower Systems

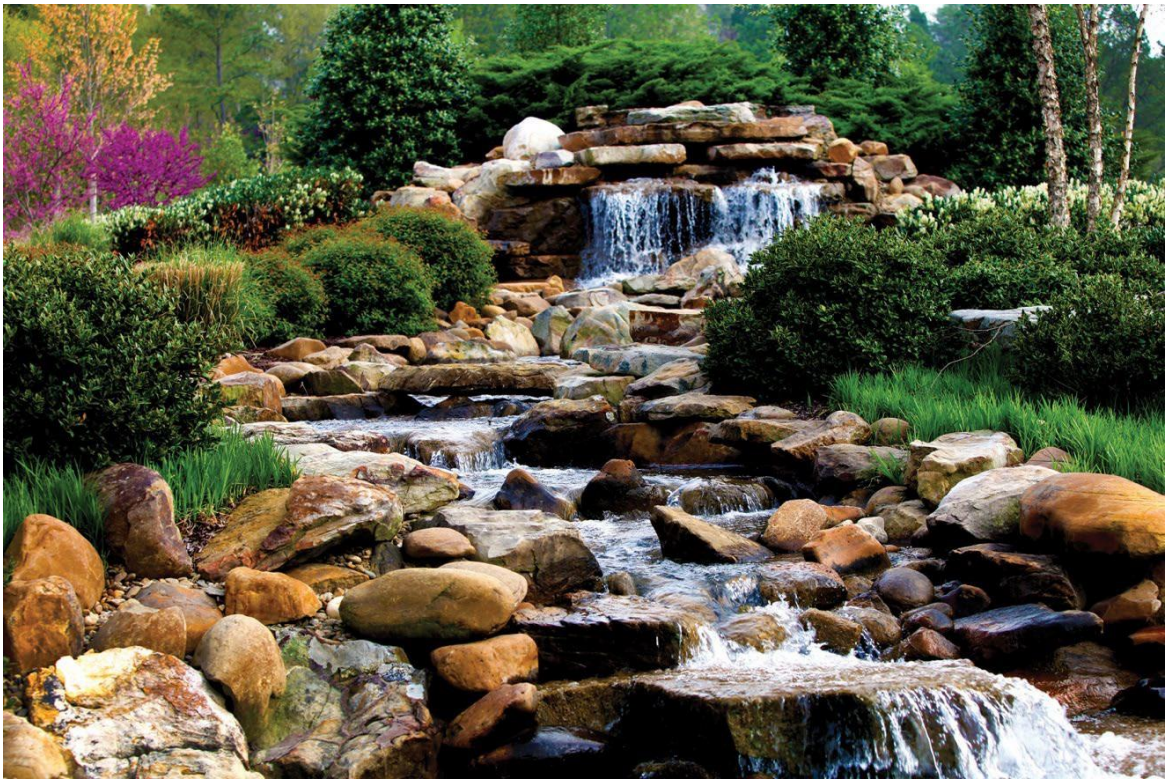

Kevin Robb
Nolan Goth
Ethan Kappes
Xin He
Jun Qu

November 2024

OAK RIDGE National Laboratory

ORNL IS MANAGED BY UT-BATTELLE LLC FOR THE US DEPARTMENT OF ENERGY

ORNL/SPR-2024/3714
CPS 36805

Nuclear Energy and Fuel Cycle Division

DEVELOPMENT OF HIGH-TEMPERATURE (>700°C) MOLTEN SALT PUMP TECHNOLOGY FOR GENERATION 3 SOLAR POWER TOWER SYSTEMS

Kevin Robb
Nolan Goth
Ethan Kappes
Xin He
Jun Qu

November 2024

Prepared by
OAK RIDGE NATIONAL LABORATORY
Oak Ridge, TN 37831
managed by
UT-BATTELLE LLC
for the
US DEPARTMENT OF ENERGY
under contract DE-AC05-00OR22725

Final Technical Report (FTR)

Project Title:	Development of High-Temperature (>700°C) Molten Salt Pump Technology for Generation 3 Solar Power Tower Systems
Project Period:	04/01/20–5/30/23
Recipient:	Oak Ridge National Laboratory
Address:	1 Bethel Valley Rd. Oak Ridge, TN 37830-6167
Website (if available)	www.ornl.gov
Award Number:	CPS 36805
Project Team:	Oak Ridge National Laboratory
Principal Investigator:	Kevin Robb, R&D Staff Phone: 865-576-4730 Email: robbkr@ornl.gov
Technology Manager:	Rajgopal Vijaykumar
Project Officer:	Christine Bing

_____ _____

Signature **Date**

Executive Summary:

Bearings are required for long-shafted pumps historically used in concentrating solar thermal power applications. For molten chloride salts, bearings for such service conditions are not commercially available, nor has a design been demonstrated to work. Therefore, a project was sponsored by the Department of Energy's Solar Energy Technologies Office for the development and demonstration of a submerged bearing for use in chloride salt pumps. This project's tasks covered the tribological testing of candidate materials and the design, fabrication, testing, and post-test analysis of full-scale salt-compatible bearings.

This work expands upon previous work. The effects of potential particulate in the salt were investigated through tribological bench testing. Through 11 tests, the MgO particulate size and concentration in a molten chloride salt were varied, and the effects on friction, wear rate, and wear characteristics were recorded. Novel journal bearings for chloride salt service were designed and fabricated based on these results. The bearings were of a relevant scale (i.e., for a 1.5 in. pump shaft) to demonstrate the technology with respect to further scale-up. The bearings were made of Haynes 244 and Yttria Partially Stabilized Zirconia. A custom bearing test rig, salt tanks, and associated infrastructure (e.g., heaters, tanks, transfer lines, gas flow control) were designed, procured, and installed. A few issues were encountered in the system fabrication process, resulting in delay of the project schedule. The system was successfully fabricated and assembled. Heating, cover gas, and pump motor systems were integrated into the control logic. This progress of the bearing test system represents a significant step forward towards demonstrating this promising technology. Nevertheless, the project ended before testing of the full-scale bearings could be performed.

Acknowledgements:

Dan Barth and William Nagle of High Temperature System Design provided invaluable subject matter expertise and effort into the design of the prototype bearing, test rig development, and initial water shakedown studies.

This material is based upon work supported by the U.S. Department of Energy's Office of Energy Efficiency and Renewable Energy (EERE) under Solar Energy Technologies Office (SETO) Agreement Number 36805 and under contract DE-AC05-00OR22725 with Oak Ridge National Laboratory, managed by UT-Battelle, LLC.

Contents

Contents 5
Background 6
Project Objectives 7
Summary of Tasks 7
Project Results and Discussion Material Downselection 10
Task 1: Tribological Bench Testing 12
Task 1.1: Particle Size Selection 13
Task 1.2: Quantify the Friction Coefficient 14
Task 1.3: Energy-dispersive spectroscopy spectra & mappings of disc surface 14
Task 1.4: Mass and Volumetric Wear Rates 15
Task 2: Bearing and Test Rig Design and Procurement 16
Task 2.1: Mounting plate design 16
Task 2.2: Bushing and sleeve design 17
Task 2.3: Test rig design 21
Task 2.4: Review and approve drawings 23
Task 2.5: Bearing and test rig fabrication 23
Task 2.6: Pump characterization tests in water 25
Task 3: Test Rig Setup 27
Task 3.1: Support structure 27
Task 3.2: Electrical supply 28
Task 3.3: Instrumentation and control 29
Task 3.4: Thrust bearing cooling system 33
Task 3.5: Salt crucibles 34
Task 3.6: Assembly of major supporting components 35
Task 3.7: Integrate the bearing test rig 36
Task 3.8: Salt purification Task 3.8.1: Procure 39
Task 3.9: Disassembly equipment 40
Task 3.10: Cold leaking testing 40
Task 3.11: Hot leak testing 40
Task 4: Bearing Testing 40
Significant Accomplishments and Conclusions 41
Inventions, Patents, Publications, and Other Results 42
Path Forward 42
References 44

Background

Concentrating solar thermal power (CSP) converts energy from sunlight into thermal energy to drive turbine generator sets for electrical production or for direct process heat applications such as desalination and oil refinement. This renewable power technology is deployed internationally. Nitrate salt working fluids are the state of the art, and the 2016 Concentering Solar Power Gen3 Demonstration Roadmap [1] identifies higher-temperature operation as a key metric for reducing the cost per kilowatt-hour (electrical).

Molten chloride and carbonate salts were identified as leading salts for the liquid pathway. Of the two, chloride salts have several advantageous properties and are relatively cheap (e.g., low melting temperature, low viscosity, high heat capacity, and low vapor pressure). The Solar Energy Technologies Office (SETO) within the Department of Energy's Office of Energy Efficiency and Renewable Energy sponsored the demonstration of a versatile, high-temperature (>700°C) molten chloride salt facility designed to enable a variety of testing in support of the Gen 3 CSP molten salt pathway through a project named "Enabling High-Temperature Molten Salt CSP through the Facility to Alleviate Salt Technology Risks (FASTR)" [2, 3, 4]. FASTR, along with several parallel projects, has accelerated the development of molten chloride salt technology for next generation CSP. These developments contributed to the conceptual design of a 2 MWth pilot plant [5].

At the start of the FASTR project, limited pumps had been operated in molten chloride salt. FASTR chose a cantilevered centrifugal-type pump design that uses a noncontacting, gas-lubricated shaft seal with the shaft bearings positioned outside the molten salt environment. Compared with chloride salt service, short-shafted pumps (i.e., cantilevered impeller with no salt-wetted bearings) have a more extensive track record in molten fluoride salt system service [6]. Although short-shafted pumps can be used successfully, the 2 MWth pilot plant concept [5] and future scale-up of the technology call for bearing-supported long-shafted pumps. These types of pumps have been used in current nitrate salt CSP plants [7]. However, the salt-wetted journal bearings required for long-shafted pumps have not yet been developed for or demonstrated in molten chloride salts.

A previous project laid the foundation for the development of chloride salt-wetted bearings [8]. First, a literature review and consultation with bearing manufacturers was conducted to identify potential materials for bearing wear and rotary surfaces for use in a high-temperature chloride salt environment. Corrosion screening tests were then completed for 10 candidate materials at 750°C for 500 h in a prototypical chloride salt at Oak Ridge National Laboratory (ORNL) [9]. Finally, 13 pin-on-disc tribology tests were conducted in 750°C chloride salt [10]. This led to the downselection of six material pairings: silicon nitride or zirconia paired with Tribaloy T900, Haynes 244, or Hastelloy C276. In addition to the material downselection, efforts were initiated to design prototype bearings and an apparatus to test them under prototypical conditions. However, the project was halted before the bearing or test rig designs could be completed.

From this foundation, the project that is the subject of this report was initiated to further investigate salt-wetted journal bearings to further develop high-temperature molten salt pumping technology. The demonstration of this novel bearing configuration in a molten chloride salt environment will enable the development and operation of long-shafted pumps for CSP and other thermal energy storage tanks.

Project Objectives

This project was focused on the development and demonstration of a submerged bearing for use in chloride salt pumps for Gen 3 CSP plants. The primary objective of this project was to make recommendations for a salt-submerged bearing type and materials to be used in a Gen 3 CSP pump design. The recommendations were to be derived from data collected from a thorough bearing test campaign in which a chloride salt bearing test rig (designed and built as part of this project) would be used.

This project will advance the technology readiness of long-shafted molten salt pumps that require support along the shaft length submerged in the salt. Clean energy producers such as CSP plants, thermal energy storage facilities, and nuclear fission plants can significantly benefit from this innovation because it enables pumping within tall vessels. Furthermore, the research supports the future scale-up of salt pumps to sizes that necessitate a salt-wetted bearing to support the shaft.

Summary of Tasks

Tribological bench testing and prototypical bearing testing tasks were required to meet the project objective of making bearing material recommendations. Candidate bearing material combinations were downselected (based on prior corrosion test results at ORNL) for tribological bench testing [Task 1]. Tribological tests at 750°C in chloride salt were completed for seven material combinations. These tests were used to investigate the effects of impurities in the salt by adding various sizes and concentrations of MgO particles. Salt-wetted bearings and a bearing test rig were designed based on these test data [Task 2]. Existing infrastructure at ORNL was modified and extended to support the setup and operation of the bearing test rig [Task 3]. Finally, operation of the bearing test rig with the salt-wetted journal bearings [Task 4] would produce the data needed to make recommendations of bearing materials to be used in long-shafted pumps. 1 provides a summary of the project tasks. Table 2 summarizes project milestones, success criteria, and target end dates for the project.

Table 1. Summary of project tasks

Num.	Task name	Task actions
1	**Tribological bench testing**	Tribological bench testing was used to investigate the effects of particle impurities on wear. The testing used the pin-on-disc method at temperatures up to 750°C in the chloride salt. The test matrix included three different particle sizes and three different particle concentrations. A total of 11 tribological tests were performed in Task 1.
2	**Bearing and test rig design and procurement**	This task finalized the test rig design and bearing design to test full-scale bearings in a prototypical environment. This task also included the procurement of required components. Two sets of three bearings were sourced. A GO/NO-GO decision point was included. The test rig and bearing procurement cost estimate and schedule were acceptable to SETO with a GO decision.

Num.	Task name	Task actions
2.1	Mounting plate design	A mounting plate was designed so that the test rig could interface with existing molten salt tanks at ORNL.
2.2	Bushing and sleeve design	CFD models of the molten salt flow within the bearings and test rig were developed to estimate mass flow rate, velocity, and pressure drop. These models also confirmed that bearing lubrication remained uniform with the offset diffuser design. This offset design choice was made to induce a radial load on the bearings.
2.3	Test rig design	The test rig was designed to accommodate the bushing and sleeve, along with the pump impeller, shaft, motor, and seals.
2.4	Review and approve drawings	3D CAD models and engineering drawings were developed by the subcontractor. ORNL had design authority to review, approve, and sign before procurement and fabrication began.
2.5	Bearing and test rig fabrication	Fabrication of the bearing test rig components was led and organized by the subcontractor. ORNL held recurring status meetings with the subcontractor to receive updates.
2.6	Pump characterization tests in water	Before shipping the test rig to ORNL, the subcontractor performed testing in water to confirm operation and quantify pumping performance.
3	**Test rig setup**	This task was focused on the installation of the test system. This included ensuring that power, instrumentation and control systems, tanks, and salt were ready for testing. A milestone based on successfully maintaining hermetic sealing and temperature was included.
3.1	Support structure	A structure to support the test rig was designed and fabricated. The focus was minimizing vibration, enabling thermal expansion, and facilitating the ability to control the consequences of bearing failure if it were to occur.
3.2	Electrical supply	Electrical supplies for 120, 208, and 480 V circuits were extended from ORNL's main panel to the experiment setup. A heater control cabinet and an instrumentation I/O cabinet were also designed, fabricated, and installed.
3.3	Instrumentation and control	This task involved setting up all sensors and instrumentation relevant for testing and monitoring the salt-wetted journal bearings.
3.3.1	Pressure	Inlet and outlet gas mass flow controllers were equipped with digital pressure transducers. A backup set of analog pressure gauges was installed on the inlet gas lines. Adequately sized pressure relief valves were also installed as safety devices to protect equipment and personnel.
3.3.2	Temperature	Temperature monitoring was achieved with more than 50 type N and type K thermocouples. Monitored quantities included tanks, pipes, jacket heaters, immersion heaters, cover gas plena within the tanks, and several positions within various molten salt volumes.
3.3.3	Level	The salt level within the system was monitored using profile probes. Each probe had several temperature sensing points, which enabled a distributed measurement along a single axis.
3.3.4	Mass flow	Mass flow controllers, along with a pressure differential between parts of the system, enabled pneumatic transfer of molten salt without the use of traditional mechanical pumps. Supplied with a high-purity source of argon, the controllers also maintain a positive pressure and cover gas within the salt-containing tanks.
3.3.5	Vibration	Accelerometers and high-frequency data logging hardware were selected to monitor the bearing rig's performance. Degradation of the bearings can be observed with the time-dependent signal from the accelerometers. Excessive wear increases the radial gap between the shaft sleeve and the outer bushing. This increased radial gap reduces hydrodynamic stability and thus causes excess shaft movement and vibration.
3.3.6	Current draw	Experimentation with first-of-a-kind salt-wetted bearings involves the possibility of bearing degradation or eventual failure. Therefore, the motor current draw was monitored to quantify any increased rotation resistance.
3.3.7	Pump motor control	A variable frequency drive was installed to control the test rig motor direction, start/stop, rotation rate, and acceleration. The drive was supplied with 480 V of 3-phase AC and was connected to the pump motor. Signal I/O was routed to the FlexIO instrument control cabinet.

Num.	Task name	Task actions
3.3.8	Pump rotation rate	A remote optical laser sensor and frequency to analog converter/tachometer were set up to quantify the actual shaft rotation rate.
3.3.9	Heaters and insulating jackets	Trace, jacket, cartridge, and immersion heaters were used. Trace heaters were wrapped along piping segments for transfer operations. Jacket heaters encompassed the sides of the tanks to provide axial zoning. Cartridge heaters were installed within the base plates underneath the tanks. Immersion heaters enabled heating of the salt from the interior to accelerate the melting process.
3.3.10	Programable logic controllers	The control modules within the FLEX-3 control cabinet were interfaced with Allen-Bradley FactoryTalk and Studio5000 industrial automation software. Several screens of a graphical user interface were created for heater power management, loop level control, loop temperature control, etc.
3.4	Thrust bearing cooling system	A commercial-off-the-shelf thrust bearing was used to axially confine the shaft. An active gas cooling system was needed to maintain the thrust bearing below its temperature limit. A once-through flow of argon gas was selected and vented to the FASTR purification enclosure.
3.5	Salt crucibles	A set of UNS S31600 salt-wetted crucibles was fabricated because corrosion tests yielded unfavorable results with chloride salts and Nickel 201. These containers serve the function of containing the molten salt while being an easily replaceable liner for the larger pressure-rated vessels that surround them.
3.6	Assembly of major supporting components	Assembly consisted of positioning the base plate heaters, installing a spring-loaded base to enable thermal expansion of the bearing test rig, performing lifting operations to position the tanks, wrapping the tanks with heating jackets for axial temperature zone control, and insulating jackets to minimize heat loss.
3.7	Integrate the bearing test rig	Integration of the bearing test rig with the facility involved shipping, receiving, unpacking, inspecting, lifting, and sealing operations.
3.8	Salt purification	Salt purification involved procuring and purifying the required molten salt.
3.8.1	Procure	Approximately 200 kg of anhydrous carnallite salt was received from Israel Chemicals Ltd. Sufficient quantities of the Silver Peak halite salt from Albemarle Inc. are also on hand. The combination of these two products yields the desired ternary Gen 3 CSP $MgCl_2$-KCl-NaCl salt.
3.8.2	Salt transfer system	The existing purification system for FASTR was intended to be used. Salt transfer tubing was designed and procured to enable transfer of purified salt from the purification enclosure to the bearing test rig storage tank.
3.8.3	Purify salt	Salt purification was scheduled to be the last task of the facility setup. Because of project time and budget constraints, this task was not initiated.
3.9	Disassembly equipment	Consideration was made in the bearing test rig's design to aid in disassembly so that the planned disassembly and inspection tasks could be completed. Equipment consisted of a cantilevered frame for accessing the test rig, a wash tank, ultrasonic equipment, and hot work permits for any potential torch activities.
3.10	Cold leak testing	Pressurized cold leak testing of the storage tank and pump tank was completed. The storage tank held a constant pressure for 24 h, indicating that the main flange seal and access port seals were functioning properly. A pinhole leak was identified in the bearing test rig around a fillet weld sealing a penetration for the thrust bearing active cooling. After being repaired, the tank held a constant pressure for 24 h, indicating that the main flange seal and access port seals were functioning properly.
3.11	Hot leak testing	Hot leak testing was not performed.
4	**Full-scale bearing test**	Bearing Tests 1 and 2 were not performed.
4.1	Test 1	The Test 1 plan was to run continuously for 500 h, filter and drain the salt, dissemble the rig, analyze the salt for impurities, and inspect the bearings.
4.2	Test 2	Test 2 plan was left undefined and was to be driven by the outcome of Test 1.

Table 2. Project milestones, success criteria, and target end dates for the project

Milestone# GO/NO-GO	Milestone name/description	Criteria	End date	Milestone type: QPMR or AMR
M1.1	Complete tribological testing	1. Total wear volume 2. <1 × 10^{-6} mm^3/Nm 3. Two repeat measurements	9/30/2020	Quarterly progress measure (regular)
GNG2.1	GNG test rig and bearing procurement	1. Cost estimate and schedule acceptable to SETO	8/30/2021	GO/NO-GO
M2.1	Test rig drawings are approved	1. Approval of drawings	11/31/2021	Quarterly progress measure (regular)
M3.1	Vessels are ready for test rig	1. Maintain temperature 2. Remain at 700°C ±5°C for 24 h 3. 10 measurements/h	9/30/2022	Quarterly progress measure (regular)
M3.2	Test rig is assembled and ready	1. Leak rate 2. <1 × 10^{-4} scc/s helium leak rate 3. Five measurements	11/30/2022	Quarterly progress measure (regular)
M4.1	Post full-scale bearing test analysis	1. Corrosion depth 2. <1.5 mil/y (<38.1 µm/y) 3. Three measurements	3/31/2023	Annual milestone (regular)
		1. Total wear volume 2. <1 × 10^{-6} mm^3/Nm, to be updated based on bearing design 3. Three measurements	3/31/2023	Annual milestone (regular)
		1. Out of roundness 2. To be updated based on bearing design (e.g., 5% change over test duration) 3. T-Test shows 95% confidence, based on three measurements	3/31/2023	Annual milestone (regular)

Project Results and Discussion

Material Downselection

As noted in the Background section, previous efforts to identify candidate bearing materials included a literature review, static corrosion testing, and pin-on-disc tribological testing. These efforts led to the downselection of five materials (i.e., silicon nitride, zirconia, Tribaloy T900, Haynes 244, and Hastelloy C276).

A single material pairing had to be selected for the scope of the current project. Differential thermal expansion between materials is a key engineering consideration for the development of practical “full-scale” bearings. This challenge is encountered in two

areas: the area where the bearing is mounted to the pump and in the small clearance between the sleeve and the bushing of the journal bearing.

Of the five candidate materials, pairings of ceramic-on-ceramic, metal-on-metal, and metal-on-ceramic could be made. The previous pin-on-disc test of zirconia-on-zirconia resulted in an order of magnitude greater wear of the pin than that of the ceramic-on-metal pairings, discouraging further consideration of ceramic-on-ceramic pairings [10]. Molten salts are used as fluxing agents (i.e., they remove oxides from metal surfaces). Metal-on-metal contact has resulted in cold-welding and galling in various molten halide salt experiments. The concern over such phenomena occurring in a bearing discouraged further consideration of metal-on-metal journal bearing configurations. Therefore, metal-on-ceramic pairings were downselected for further development.

Depending on the material pairing, the gap between the sleeve outer diameter and the bushing inner diameter can increase or decrease substantially as the bearing is heated from room temperature to operating temperature. Two example cases are provided for material pairings of silicon nitride with 316 stainless steel and zirconia with Haynes 244 to illustrate this challenge:

> Example 1: Silicon nitride has a uniform mean coefficient of thermal expansion of approximately 3.1 µm/m°C. By contrast, 316 stainless steel has a mean coefficient of thermal expansion of 18–19 µm/m°C in the operating temperature range of interest. Assuming that a journal bearing with a radius of 1 in. (25.4 mm) is used, the differential thermal expansion from room temperature to 725°C would be 260 µm (0.010 in.). For an order-of-magnitude comparison, a typical radial clearance for this size bearing is 25–50 µm. Thus, the change in the gap as a result of differential thermal expansion from room temperature to the operating temperature is approximately 5–10× the nominal gap.
>
> Example 2: Relative to other ceramics, Zirconia has a high mean thermal expansion coefficient (i.e., approximately 10.3 µm/m°C). Conversely, relative to many metals, Haynes 244 has a low mean thermal expansion coefficient of 12–13 µm/m°C in the operating temperature range of interest. Assuming that the same journal bearing with a radius of 1 in. (25.4 mm) is used, the differential thermal expansion from room temperature to 725°C would be 46 µm (0.0018 in.).

Although the change in the radial gap for the zirconia with Haynes 244 is substantial, it is 5.6× less than that of the silicon nitride with 316 stainless steel pairing example. In addition to the change in radial gap where the fluid resides, differential thermal expansion presents similar challenges to mounting the bearing in the pump.

The material pairing was downselected based on the previous test campaign [10], material sourcing, and mechanical properties. Haynes 244 and zirconia were chosen (yttria partially stabilized tetragonal zirconia polycrystal, YTZP obtained from Ortech).

Task 1: Tribological Bench Testing

The MgO particulate can be present in the salt because of the thermal decomposition of MgO-HCl and/or direct reaction of $MgCl_2$ with moisture and hydroxide impurities. The presence of MgO particulate in the salt was identified as a concern for the wear and ultimate performance of salt-wetted bearings. Before this project, no literature existed on the effects of MgO on the system of interest. Thus, this task sought to generate first-of-a-kind data and insight for the effects of MgO on the tribological performance of wear materials in the NaCl-KCl-$MgCl_2$ ternary salt of interest.

Tribological testing involved the use of an existing Advanced Mechanical Technology, Inc. high-temperature pin-on-disc tribometer at ORNL. This tribometer was modified to accommodate the 750°C chloride salt, as shown in Figure 1. The friction between the two materials was recorded in situ, and the materials were checked for indications of scuffing or galling. Post-test worn surface morphology examination and composition analysis provide information necessary to understand the failure modes (if failed) and provide direction for improvement (if promising). The same experimental setup and chloride salt purification procedures were used in the preceding tribological testing [10].

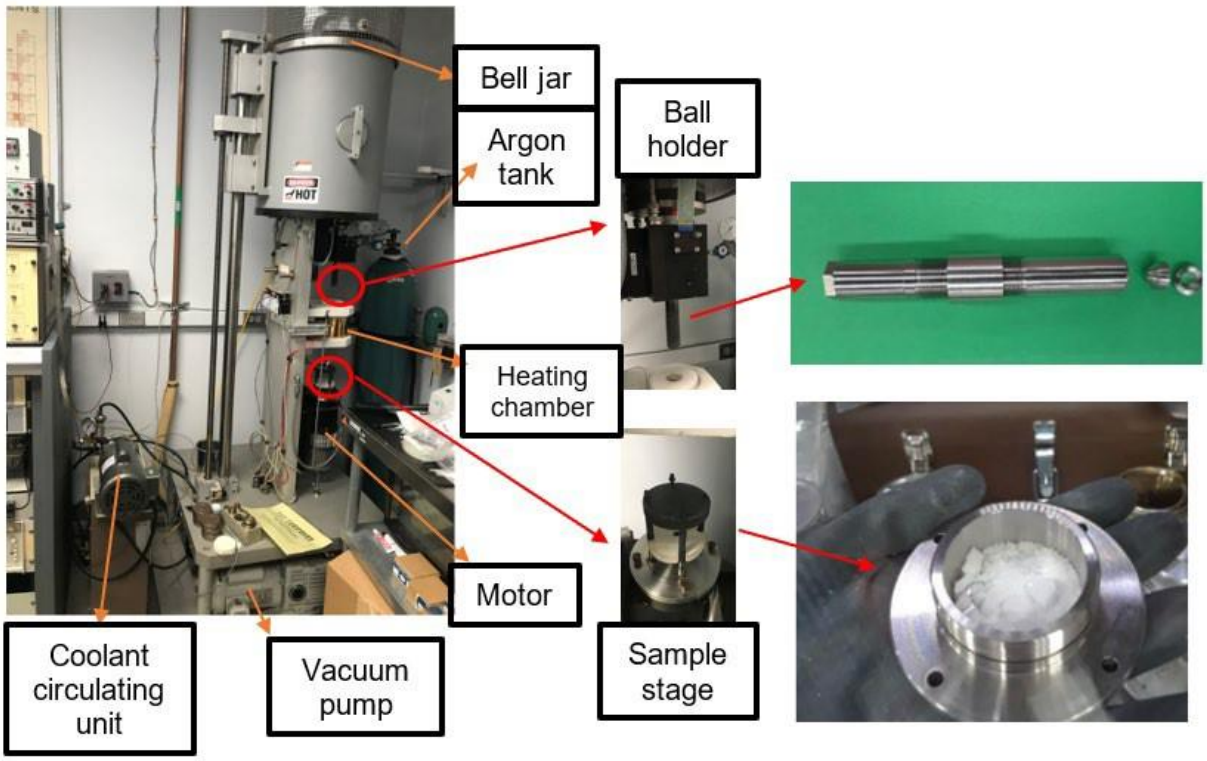

Figure 1. Pin-on-disc tribometer experimental setup.

Tribological bench testing was used to investigate the effects of particle impurities on wear. The testing used the pin-on-disc method at temperatures up to 750°C in the chloride salt. The test matrix included three different particle sizes and three different particle concentrations. A total of 11 tribological tests were performed in Task 1. The work and findings are reported in a journal paper (noted in referenced literature [11]).

The results of Task 1 are summarized as follows:

- Eleven tribological bench tests were successfully completed.
- When the concentration of MgO particles used was 0.3 wt %, the wear losses on the ceramic balls increased with particle size, whereas the wear losses on the alloy discs remained almost unchanged. The presence of particles could effectively peel off the material from the zirconia ball surfaces which facilitate the adhesive wear. The coverage of the adhesion substance became larger with larger-sized particles.
- A higher concentration of MgO particles made wear on the alloy disc surfaces more significant. The initial abrasive wear on the alloy discs is suspected to have been more severe with more particles at the interfaces.
- Shear-induced hardening was observed inside the wear tracks, which increased in hardness by approximately 10–20%. The presence of MgO particles can facilitate this process.

Task 1.1: Particle Size Selection

Researchers at the National Renewable Energy Laboratory (NREL) conducted a series of tests to quantify the potential concentration and size distribution of the MgO in the ternary salt of interest after purification; as well as due to impurity (air and moisture) ingress [12]. Their results indicated that the presence of MgO was approximately 0.03 wt % (mass fraction) and that presence of MgO-HCl, which can thermally decompose to produce MgO, was 0.09–0.17 wt %. The size distribution ranged from approximately 0.3 to 300 µm with a broad peak around 10 to 30 µm.

NREL's pioneering work provided key insight into the potential concentration and size distribution of MgO. However, some uncertainties and questions remain regarding the conditions that could be encountered in the pumps of a full-scale CSP system:

- Are there system scale effects (e.g., 50 g salt scale tests vs. 10,000+ ton salt scale CSP plant, initial salt impurities) that affect the concentration of MgO particulate that could be encountered at the pump?
- How does MgO size distribution and concentration evolve over time (e.g., 1–21 h tests vs. 30 y of plant operation)?

Three MgO particle sizes (1–5, 37–44, and 105–149 µm) and three concentrations (0.1, 0.3, and 1.0 wt %) were selected for study based on discussions with NREL prior to the publication of Zhou's work [12]. The particles were added to the purified salt for the pin-on-disk tests. Notably, as was the case for the NREL salt, the "clean" purified salt most likely contained a baseline concentration/distribution of MgO particulate. The project team considered various means of prefiltering the salt. However, the filtering methods and additional salt handling could also add particulate to the salt. This led to the decision to add a known concentration of MgO particles to the purified salt (i.e., "spike" the purified salt).

Task 1.2: Quantify the Friction Coefficient

The following test parameters were used: 120 rpm speed, 20 N load, 1000 m distance, 750°C, and ternary salt purified using the magnesium contact procedure. These parameters were consistent with the parameters of the previous test campaign.

Figure 2 shows the friction coefficients measured in situ [11]. The MgO addition reduced the friction coefficient at the beginning of the test as a result of the particles separating the contact interface. However, the friction coefficient rose over the course of the test, arriving at values similar to those in the tests in which additional MgO was not added. The MgO particle addition also accelerated the wear loss by 3-body abrasion.

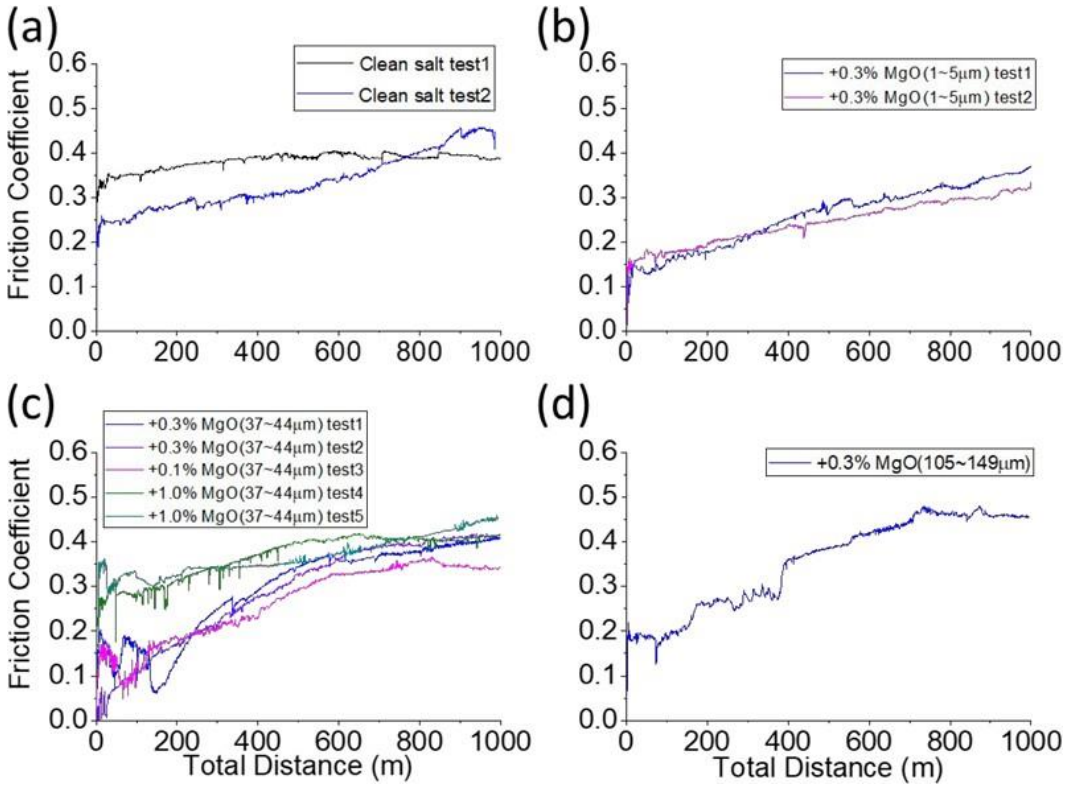

Figure 2. Friction coefficient of ZrO_2 against Haynes 244 in (a) clean salt (b) salt in which 1–5 μm MgO was added, (c) salt in which 37–44 μm MgO was added, and (d) salt in which 105–149 μm MgO was added (from He et al. [10]).

Task 1.3: Energy-dispersive spectroscopy spectra & mappings of disc surface

After the tests, scanning electron microscopy and energy-dispersive spectroscopy scans of the disc surface were conducted, as shown in Figure 3 [11]. As the particle size of the added MgO increased, the amount of zirconium detected within the wear track increased. Because zirconium is not present in the Haynes 244 disc, its presence is attributed to wear and subsequent deposition from the zirconia ball.

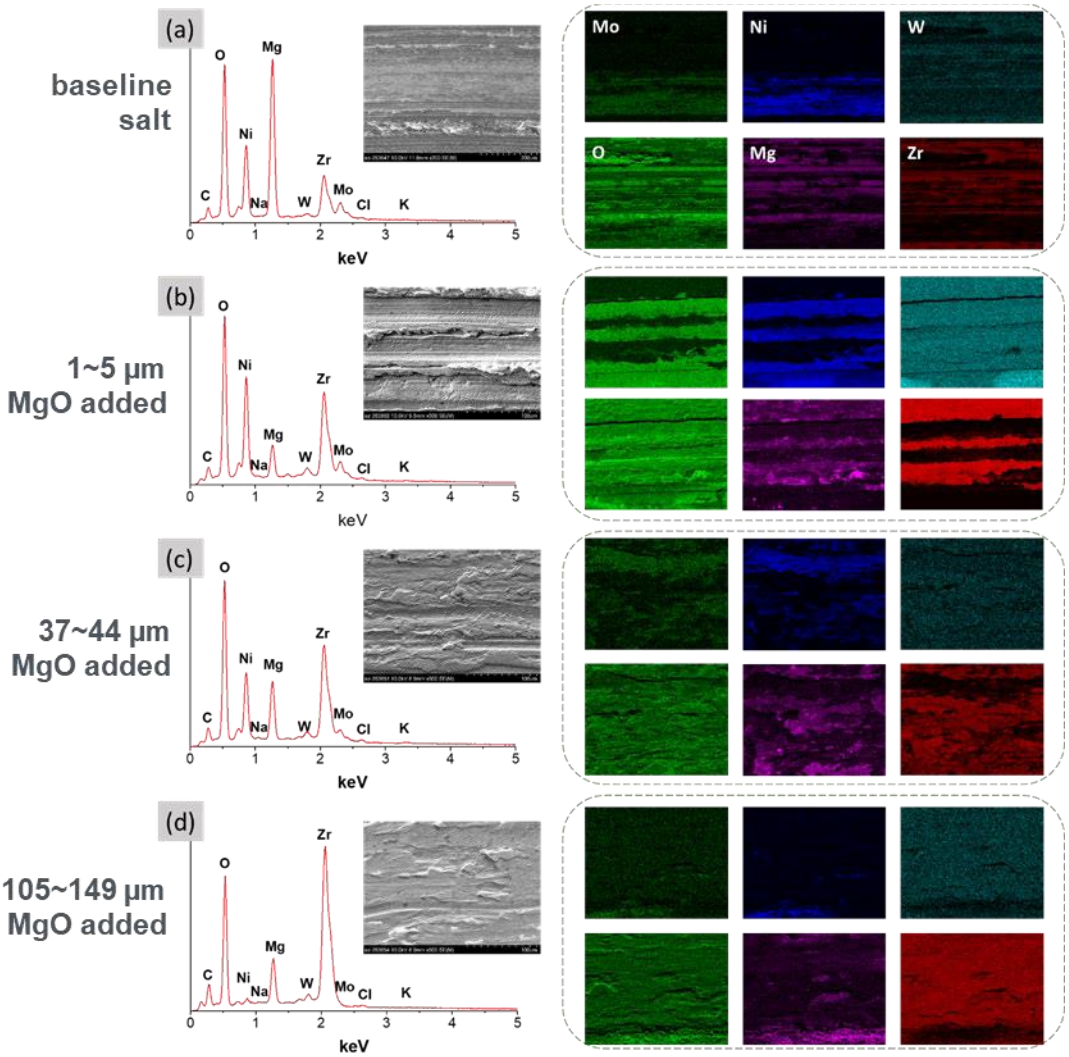

Figure 3. SEM and EDS scans of the disc wear track for tests with 0.3 wt % added MgO particles.

Task 1.4: Mass and Volumetric Wear Rates

A milestone criterion of 1.0×10^{-6} mm^3/Nm was chosen for comparison based on expert opinion and values that may be encountered in other bearing applications. As summarized in Table 3, the wear rates were higher than the chosen metric. However, all the disc wear rates were within the same order of magnitude as the metric and were deemed to have passed the intent of the metric. For the ball, the wear rates were also in the same order of magnitude for the baseline salt and with 0.1 wt % of particles added. However, at concentrations of 0.3 wt % and 1.0 wt %, the wear rate of the ball was an order of magnitude beyond the metric.

Table 3. Disc and ball volumetric wear rates for various MgO particle sizes and concentrations

MgO size (um) / Added MgO Content	Disc wear rate (Haynes 244) (1×10^{-6} mm^3/Nm)			Ball wear rate (YTZP) (1×10^{-6} mm^3/Nm)		
	1–5	37–44	105–149	1–5	37–44	105–149
1.0 wt %		5.65 ±0.25			14.15 ±0.40	
0.3 wt %	3.60 ±0.15	3.65 ±0.15	4.00	9.90 ±0.25	13.10 ±0.25	13.75
0.1 wt %		3.50			8.25	
0.0 wt % (baseline)	3.15 ±0.10			3.50 ±0.35		

Task 2: Bearing and Test Rig Design and Procurement

This task finalized the test rig and bearing design to test full-scale bearings in a prototypical environment. This task also included the procurement of required components, including two sets of three bearings.

The statement of project objectives included a GO/NO-GO decision point for the bearing test rig design and procurement. The test rig and bearing procurement cost estimate and schedule were quoted and deemed acceptable with a GO decision from the sponsor.

Several challenges affected the lead time for the test rig:

- Magnetic motor-shaft coupling of the 10 HP motor: The sponsor advised (based on previous experience) increasing the sizing of the motor to 10 HP. The magnetic coupling for this size motor was a nonstocked size that carried a long lead time.
- Yttria Partially Stabilized Zirconia (YTZP) bushing fabrication: Tooling at the vendor/manufacturer for the bushing was protracted, resulting in delayed receipt.
- Metal fabrication: The flange faces were initially out of specification, causing misalignment of the assembled test rig and issues during the first water test. These faces had to be re-machined, a process that required disassembly and reassembly of the test rig.
- Additional water shakedown testing: Because of the aforementioned issue, an additional series of shakedown tests was performed.
- Improper weld: A defect in a gas space weld was identified during pressurized cold leak testing. This defect was addressed.

Although the test rig was procured for the quoted cost, these and additional factors resulted in the lead time extending from the quoted 6 months to 18 months.

Task 2.1: Mounting plate design

A mounting plate was designed so that the test rig could interface with existing molten salt pressure vessels at ORNL. Figure 4 shows an engineering drawing of the mounting plate. Careful consideration was made to ensure dimensional and material

compatibility, and functional requirements were incorporated so that the cooling gas flow, temperature, level, and pressure could be measured.

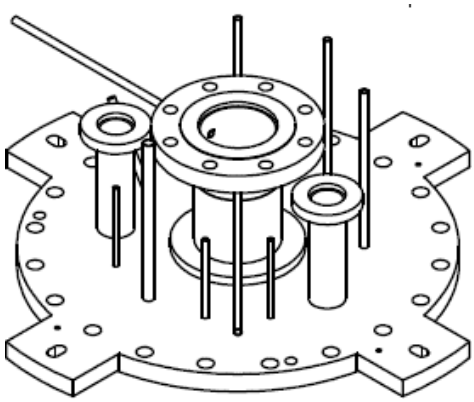

Figure 4. Illustration of the mounting plate that couples the test rig to existing ORNL vessels.

Task 2.2: Bushing and sleeve design

The salt-wetted bearings of interest (shown in Figure 5) consist of an outer bushing, a bushing holder, and an inner sleeve that is mounted to the shaft. The outer bushing is constrained within its holder, which is referred to as a spider. The material selected for the bushings was YTZP manufactured by CoorsTek. The bushing length and inner diameter are 2 in. Three helical grooves were cut into each bushing. These grooves were sized based on the chloride salt viscosity and expected velocity to ensure adequate fluid lubrication between the bushing and shaft sleeve. The grooves also provide a bypass path for MgO particles in the salt. The inner sleeve was designed to be mechanically attached to the rotating shaft with set screws. The material selected for the shaft sleeves was Haynes 244 alloy, a Ni-Mo-Cr-W alloy developed for static parts in advanced gas turbine engines that require low thermal expansion.

The design was further informed by ORNL CFD studies to quantify the (1) velocity fields, (2) pressure fields, (3) reactionary forces from impeller rotation, (4) wall shear stress, and (5) to ensure that bearing lubrication remained uniform. The offset diffuser design is shown in Figure 6. The offset diffuser was designed to place the expected radial load of full-scale pumps onto the bearings. This load ensured that the bearing wear would be prototypical for CSP and thermal energy storage applications.

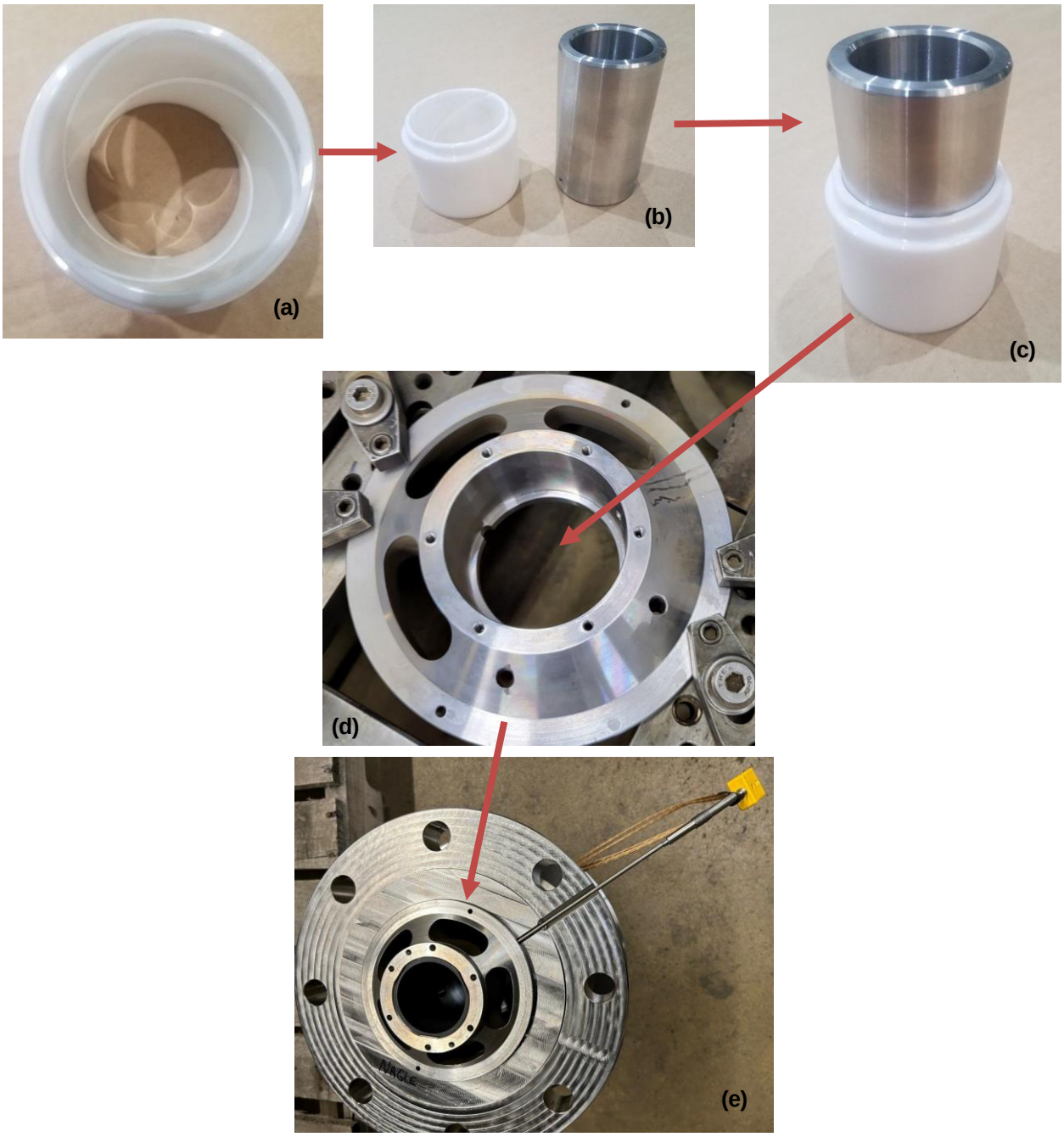

Figure 5. Bearing assembly process. (a) The outer YTZP bushing, (b and c) the addition and concentric installation of the bushing and the Haynes 244 shaft sleeve, (d) the bearing location within the spider, and (e) spider installation within the pump column assembly.

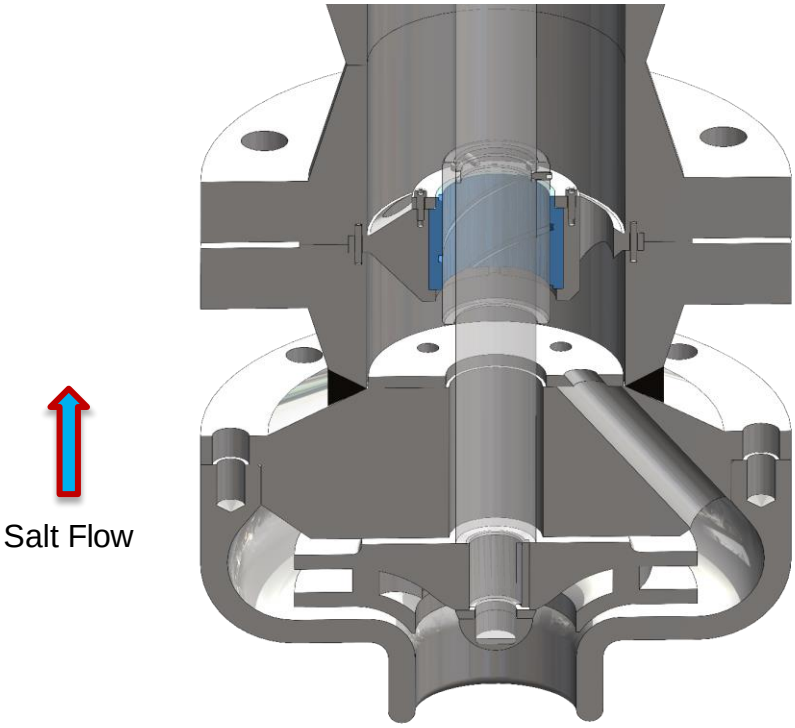

Figure 6. Offset diffuser used to induce a radial load on the bearings.

One design change from the study involved modifying the orifice plate to increase the bearing flow uniformity. Figure 7 presents the initial configuration with a single offset orifice and an improved configuration with 16 small, distributed orifices. The histograms highlight that the initial configuration resulted in Bearing 1 receiving 3% of the total mass flow and that nonuniform mass flows occurred through the three spiral grooves. Bearings 2 and 3 only received 1.5% of the total flow (50% less than Bearing 1). The improved configuration resulted in nearly equal mass flow through each bearing; each bearing received approximately 1.5% ±0.1% of the total mass flow. Additionally, the amount of salt flowing through the three grooves of Bearing 1 was improved.

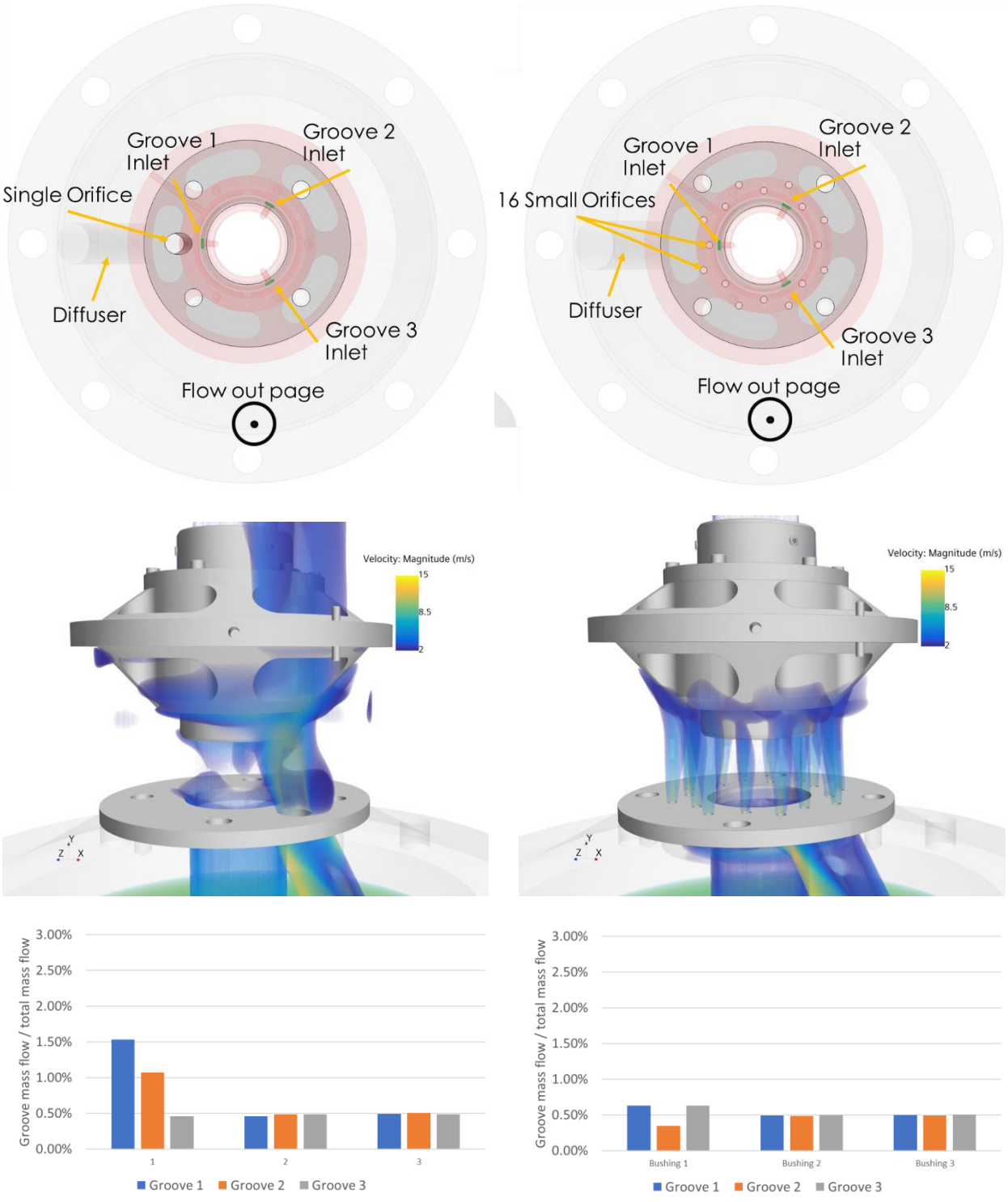

Figure 7. Offset diffuser designs with (left) one large orifice and (right) 16 small, distributed orifices. The small, distributed orifices improved bearing lubrication uniformity to the three spiral grooves of Bearing 1.

Task 2.3: Test rig design

The test rig was designed to accommodate the bushing and the sleeve, along with the pump impeller, shaft, motor, and seals. Figure 8 presents side and side cross-sectional views of the test rig. The test rig can be lowered into an open-top cylindrical pressure vessel at ORNL and rests on the main mounting flange. The molten salt flow is entrained up through the impeller and volute and is directed vertically up through a diffuser and into three bearings that surround the pump shaft. After flowing past the third bearing, the salt is turned 180° via return piping and is thus ready to be recirculated within the test rig.

The following are the primary components of the test rig:

1. Three-phase 10 HP motor (not shown)
2. Magnetic shaft coupler to avoid shaft seals
3. Instrument ports for temperature, pressure, and fluid level
4. Cooling chamber and thermal baffles to actively manage the operating temperature of a dry thrust bearing
5. Salt fill and drain connections
6. Mounting plate to interface with an existing ORNL heated salt tank
7. Return piping to direct salt downward into the liquid volume
8. Three salt-wetted journal bearings
9. Impeller and volute for entrainment and direction of salt flow

The test rig design was assessed against American Society of Mechanical Engineers (ASME) pressure vessel requirements. The COMPRESS software was used to ensure the test rig met the intent of ASME Section VIII Div. 1 .

Coupled thermal and structural finite element analysis of the test rig was also conducted, as shown in Figure 9. This demonstrated that the upper thrust bearing and mag-drive coupling temperatures and the thermally induced stresses were acceptable.

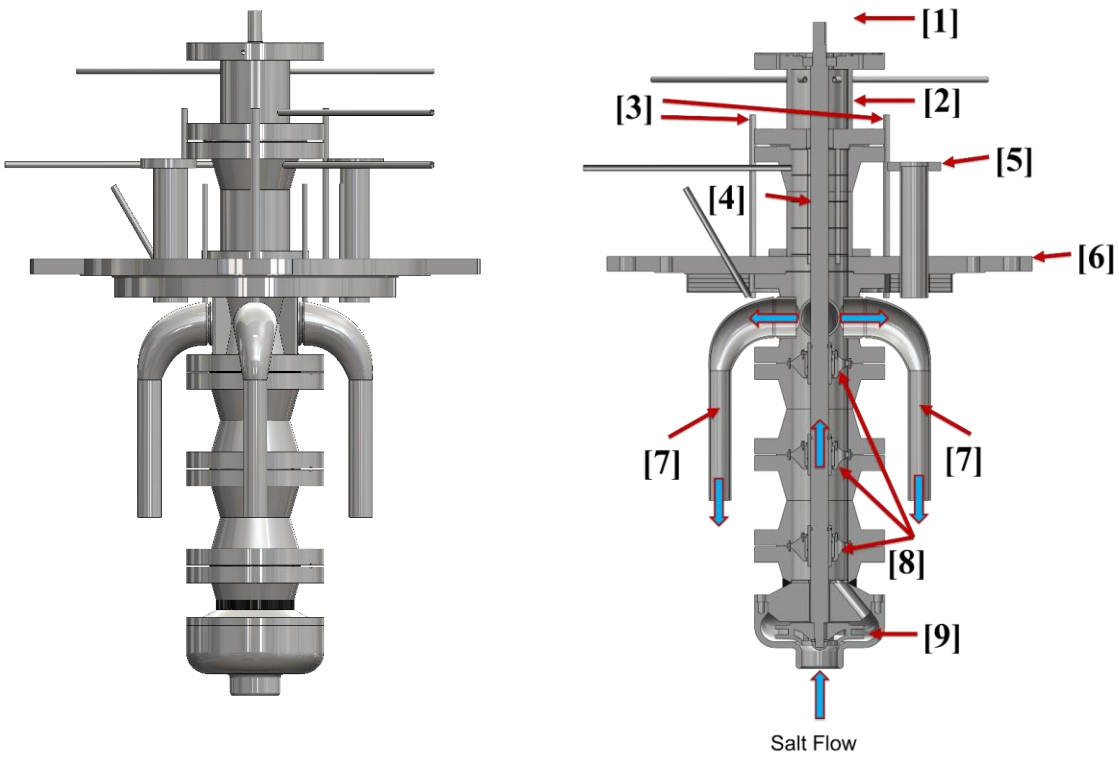

Figure 8. Side and side cross-sectional views of the test rig.

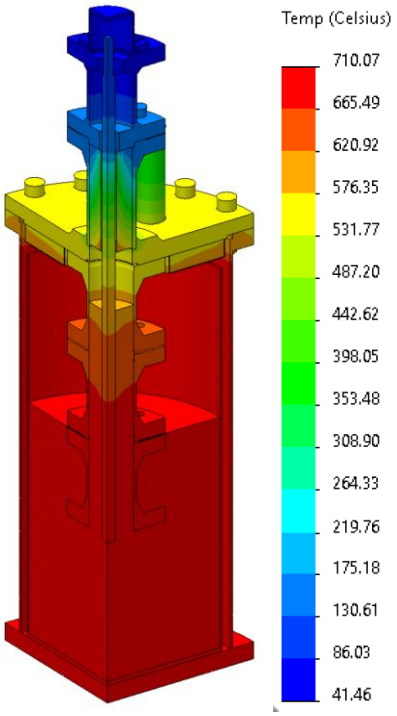

Figure 9. Example result from coupled thermal and structural finite element analysis.

Task 2.4: Review and approve drawings

The subcontractor for the chloride salt bearing testing rig provided a set of engineering drawings and 3D CAD models for review. ORNL met with the subcontractor twice per month to review progress and provide input on the design. After final review in December 2021, ORNL approved the drawings of the test rig for fabrication.

Task 2.5: Bearing and test rig fabrication

Figure 10 and Figure 11 present fabrication progress for the main mounting plate, the spider assemblies, the impeller outlet diffuser, the column assemblies, and the return piping. The salt-wetted components are primarily constructed of 316 stainless steel. The gas space pressure boundary is primarily constructed of 304H stainless steel.

The main column of the test rig was created using 5 in. 300 lb. Sch. 80 weld neck flanges (shown in Figure 11). During the first series of water tests with the assembled test rig, excess vibration was noted. This vibration was attributed to misalignment of the flange faces that form the column. The test rig was disassembled, and the flange faces were re-machined to resolve this issue. The test rig was then reassembled.

Figure 10. Fabrication progress of the (a, c) main mounting plate, (b) the bearing spider assemblies, and (d) the impeller offset outlet diffuser.

Figure 11. Fabrication progress of the column assemblies and return piping.

Task 2.6: Pump characterization tests in water

The test rig's hydraulic behavior was characterized via tests performed in water. These tests were performed by the subcontractor before the rig was shipped to ORNL. Because of the expense and long procurement time of the YTZP bushings and the Haynes 244 shaft sleeves, iron graphalloy bushings and 420 stainless steel shaft sleeves were substituted. Another motivator for the part substitution during water testing was that the YTZP and Haynes parts were fabricated with consideration for thermal expansion from room temperature to the molten salt testing temperature. Therefore, the running clearance of the iron graphalloy and 420 stainless steel parts was set to the expected clearance during hot operation of the Haynes 244 and YTZP bearings.

Measured quantities during testing included temperature, motor amperage draw, vibration, and shaft rotation rate. Table 4 and Figure 12 present the results of these tests. Figure 13 shows the test rig being installed and submerged in the water tank. The following tests were performed:

- **Test 1: Temperature, amperage, and vibration for fully wetted condition**
  - The test rig was mounted on I-beams on the top flange of the tank. The return lines were fully submerged in the water, and the upper bushing was dry. The test rig was run for 15 min at 1,200 rpm and 1,800 rpm. Motor amps and temperatures were recorded. Vibration readings were taken at each speed. A video recording was made at each speed.
- **Test 2: Temperature, amperage, and vibration for initial dry condition**
  - The water level in the tank was drained to just below the bottom bushing. The return lines at the top of the test rig were out of the water, and all three bushings were initially dry. The test rig was run for 15 min at 1,200 rpm and 1,800 rpm. Motor amps and temperatures were recorded.

Vibration readings were taken at each speed. A video recording was made at each speed.

- **Test 3: Volumetric flow rate**
  - 2 in. flex hoses were connected to the four return lines and directed into 5 gal buckets. The test rig was operated until the buckets were nearly full, and then the pump was stopped. The mass and volume of water transferred into the buckets were then quantified to establish the flow rate of the test rig at multiple rotation rates.

Table 4. Water testing results of volumetric flow rate and motor current draw as a function of the pump rotation rate

Pump rotation rate (rpm)	Volumetric flow rate (gal/min)	Motor draw ($L1_{amp}$, $L2_{amp}$, $L3_{amp}$)
600	12.0	5.3, 5.2, 5.3
900	21.5	5.8, 5.5, 5.6
1,200	48.0	N/A
1,500	N/A	6.2, 5.9, 6.2
1,800	64.0	6.7, 6.3, 6.6

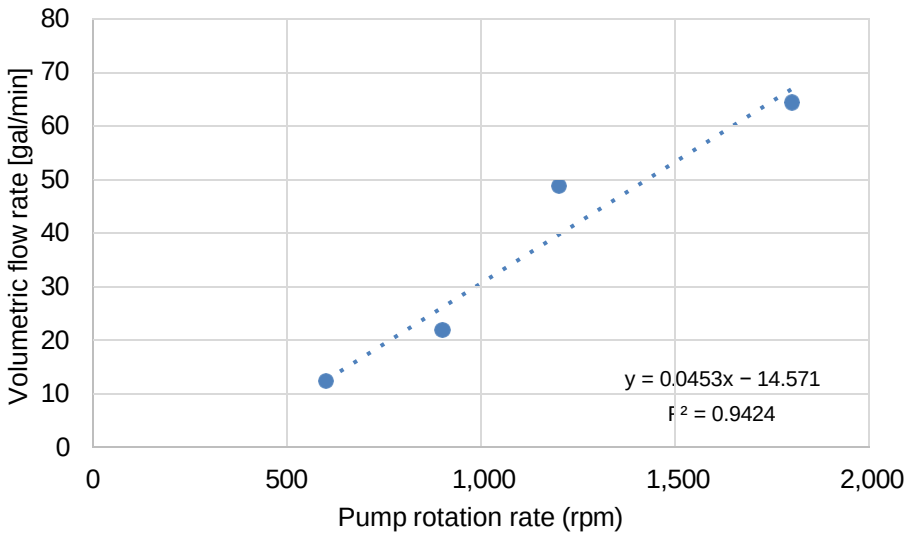

Figure 12. Volumetric flow rate and motor current draw as a function of pump rotation rate.

Figure 13. Lifting operating and water testing of the test rig by the subcontractor before the test rig was shipped to ORNL.

Task 3: Test Rig Setup

New and existing infrastructure at ORNL were installed or adapted to meet the functional requirements of testing salt-wetted bearings within the test rig. Activities included fabricating a support structure, supplying electrical power, and installing instrumentation and controls. Once the test rig was received, it was installed.

Task 3.1: Support structure

A structure to support the test rig was designed and fabricated. Design requirements included minimizing vibration, enabling dimensional growth due to thermal expansion, and facilitating the ability to control the consequences of bearing failure if it were to occur. The stand consisted of 316 stainless steel 4 in. tubing with a 0.25 in. wall frame; a 1 in. 2-piece plate to support the tank and pump at the main flange and enable assembly and disassembly of the test rig; a spring-loaded base to enable axial thermal expansion of the system; and salt drip trays (as shown in Figure 14).

Figure 14. Frame, 2-piece plate, spring-loaded base, and drip trays of the support structure.

Task 3.2: Electrical supply

Electrical supplies for 120, 208, and 480 V circuits were extended from the ORNL's main panel to the experiment setup. The 120 V circuits powered some of the control modules, mass flow controllers, and trace heaters installed on piping. The 208 V circuits powered tank base plate and jacket heaters, along with trace heaters installed on piping. The 480 V circuit was fed to the test rig pump motor. DC power supplies were installed within the FlexIO cabinet to power most of the sensors listed under Task 3.3.

A heater control cabinet was designed and installed to house the circuit breakers and solid-state relays for the various jacket and trace heaters (as shown in Figure 15). An instrument control cabinet was designed and installed to house the I/O modules for the various pressure, temperature, level, mass flow, vibration, current draw, and pump motor controls (as shown in Figure 16).

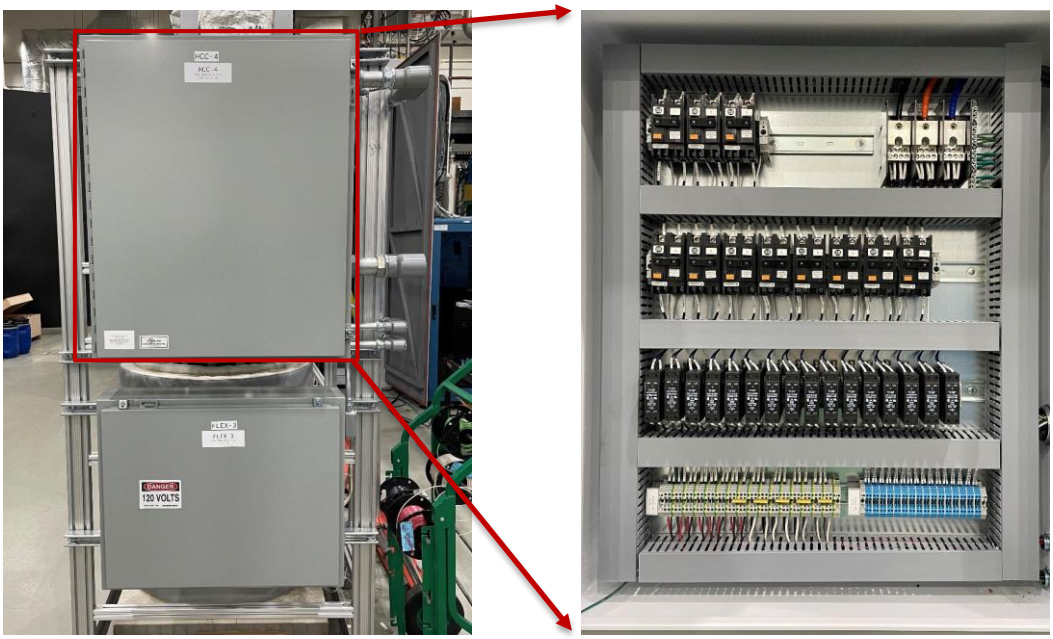

Figure 15. Electrical layout within Heater Control Cabinet #4.

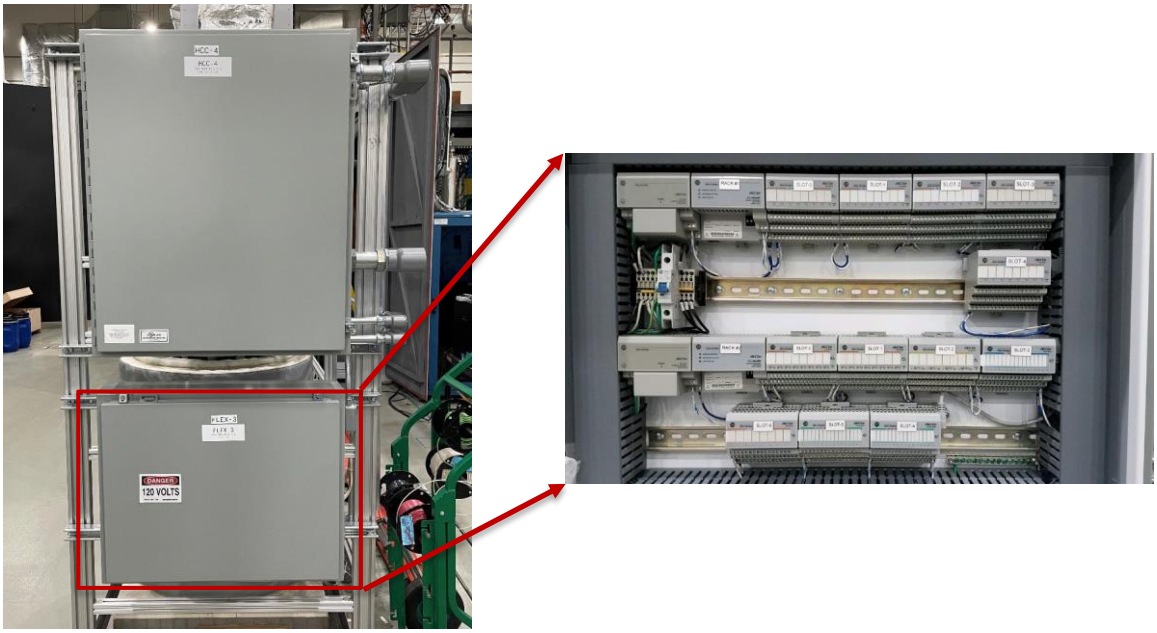

Figure 16. Electrical layout within FlexIO Cabinet #3 (FLEX-3).

Task 3.3: Instrumentation and control

Instrumentation and controls were set up for analog and digital actuation, monitoring, and data logging of several parameters. The following subsections discuss each of these items.

Task 3.3.1: Pressure

Pressure monitoring and control were needed to ensure that maximum pressure vessel limits were not exceeded during testing of the salt-wetted bearings. Pressure within the system was managed using mass flow controllers capable of either adding or reducing high-purity argon gas. Inlet gas mass flow controllers were equipped with digital pressure transducers. A backup set of analog pressure gauges was installed on the inlet gas lines. Outlet gas mass flow controllers were set up to reduce system pressure during salt flow transfers and to accommodate gas thermal expansion during heating. The outlet gas flow can be directed into the large, ventilated enclosure that houses the chloride salt purification equipment. Adequately sized pressure relief valves were also installed as safety devices to protect equipment and personnel from any pressure-related transient event.

Task 3.3.2: Temperature

Temperature monitoring was achieved with more than 50 type N and type K thermocouples. Data logging occurred at a frequency of 1 Hz. Monitored quantities included tanks, pipes, jacket heaters, immersion heaters, cover gas plena within the tanks, and several positions within various molten salt volumes. Thermocouples were also installed to monitor the bearing temperatures, as shown in Figure 17.

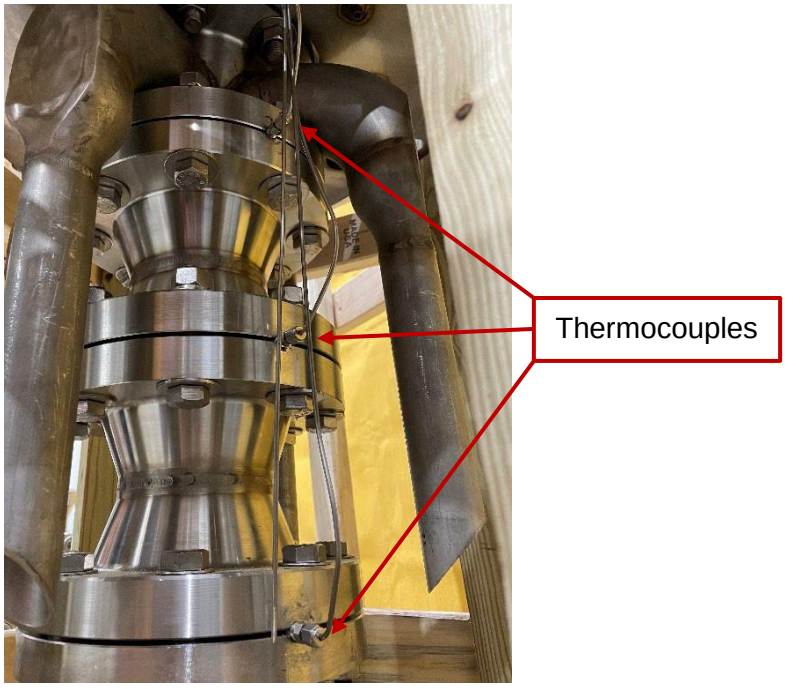

Figure 17. Compression fittings securing type N thermocouples fed through the flanges. Sensor tips were positioned up against the outer wall of the salt-wetted journal bearings.

Task 3.3.3: Level

The salt level within the system was monitored using profile probes. Each probe had several temperature sensing points, which enabled a distributed measurement along a single axis. For a nonhomogenized temperature system (e.g., transferring hot salt into a tank), the liquid level can be determined by the increase in temperature of some of the distributed sensing points along the probe.

A secondary means of level control for homogenized temperature systems was achieved by placing each tank on a mass scale. Knowing the mass, salt density, and internal dimensions of the tank enables quantification of the salt level.

Task 3.3.4: Mass flow

Gas mass flow controllers, Figure 18, along with a pressure differential between parts of the system, enabled pneumatic transfer of molten salt without the use of traditional mechanical pumps. Supplied with a high-purity source of argon, the controllers also maintain a positive pressure and cover gas within the salt-containing tanks to minimize oxidation-related issues.

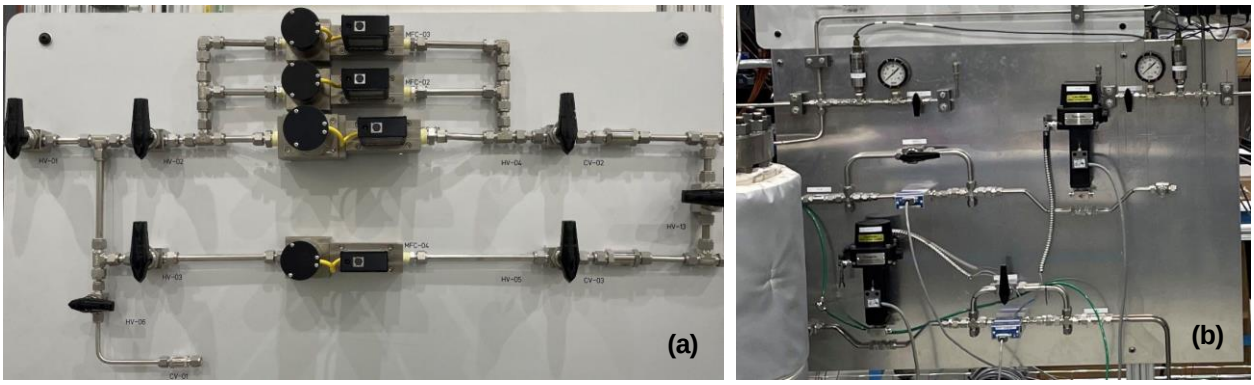

Figure 18. Routing of gas supply and return for (a) the inlet-side and (b) the outlet-side mass flow controllers.

Task 3.3.5: Vibration

Existing accelerometers and high-frequency data logging hardware were identified and selected to monitor the bearing rig's performance during its testing campaigns. Degradation of the hydrodynamic bearings can be observed with the time-dependent signal from the accelerometers. Excessive wear increases the radial gap between the shaft sleeve and the outer bushing. This increased radial gap reduces the hydrodynamic stability and thus causes excess shaft movement.

Task 3.3.6: Current draw

Another quantity of interest for the bearing rig's performance during its testing campaigns was the motor current draw. Experimentation with first-of-a-kind salt-wetted

bearings involves the possibility of bearing failure. It was hypothesized that some types of bearing performance degradation could be observed through an increased resistance to rotation. This phenomenon could be captured by monitoring the motor current draw.

Task 3.3.7: Pump motor control

A variable frequency drive was installed to control the test rig motor direction, start/stop, rotation rate, and acceleration. The drive was supplied with 480 V of 3-phase AC and was connected to the pump motor. Signal I/O was routed to the FlexIO instrument control cabinet.

Task 3.3.8: Pump rotation rate

Although the variable frequency drive can provide the demanded shaft rotation rate, it cannot provide the actual rotation rate. A remote optical laser sensor and frequency to analog converter/tachometer were set up to quantify the actual shaft rotation rate.

Task 3.3.9: Heaters and insulating jackets

Trace, jacket, cartridge, and immersion heaters were used in the effort. Trace heaters were wrapped along smaller piping segments for transfer operations. Jacket heaters encompassed the sides of the tanks to provide axial zoning. Cartridge heaters were installed within the base plates underneath the tanks. Immersion heaters enabled heating of the salt from the interior to accelerate the melting process. For each tank, there were four external zoned heaters and one internal immersion heater; there were also custom insulating jackets for each tank and lid, as shown in Figure 19.

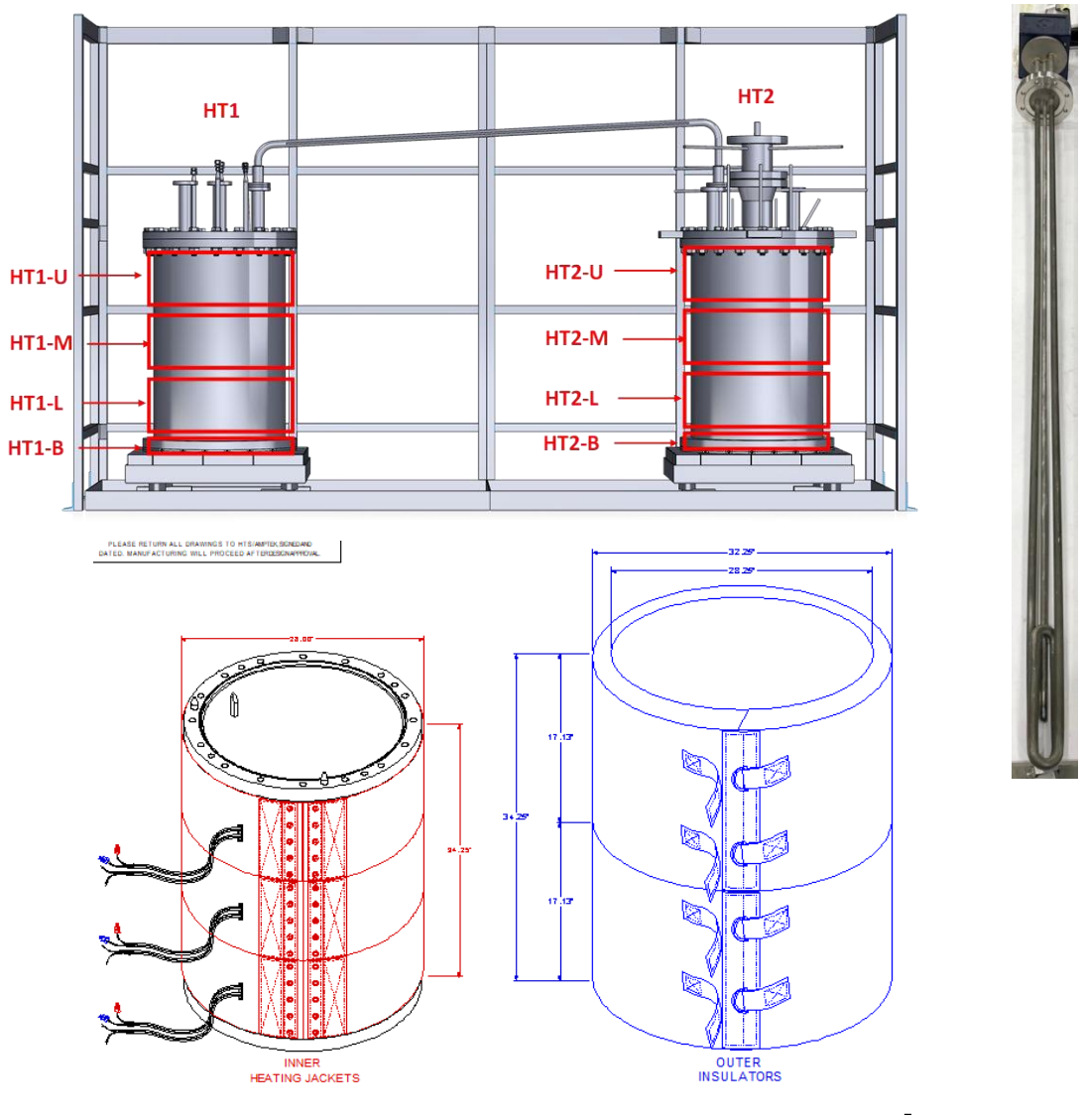

Figure 19. Jacket heaters, immersion heaters, and insulating jackets for each tank.

Task 3.3.10: Programable logic controllers

The control modules within the FLEX-3 control cabinet were interfaced with Allen-Bradley FactoryTalk and Studio5000 industrial automation software. Several screens of a graphical user interface were created for heater power management, loop level control, loop temperature control, etc.

Task 3.4: Thrust bearing cooling system

Outside the 700°C molten salt environment, a commercial-off-the-shelf thrust bearing was used to axially confine the shaft of the test rig. This thrust bearing has a maximum operating temperature of 350°C. Therefore, an active gas cooling system was needed to maintain the thrust bearing below its temperature limit. A once-through flow of argon gas was selected as the heat transfer fluid. Supply and exhaust piping routes were

designed but not installed. This exhaust gas route utilizes the large, ventilated enclosure that houses the FASTR chloride salt purification equipment.

Task 3.5: Salt crucibles

Part of the existing infrastructure at the start of this project included sacrificial Nickel 201 salt crucibles. These were originally fabricated for use with FLiNaK. The salt-wetted containers serve the function of containing the molten salt while being an easily replaceable liner for the larger pressure-rated vessels that surround them.

Chloride salt corrosion testing [4313] indicated that pure nickel and Nickel 201 coupons performed worse than desired. Therefore, a set of UNS S31600 crucibles was fabricated.

Figure 20. Salted-wetted replaceable (left) Nickel-201 and (right) UNS S31600 crucibles.

ORNL hoisting and rigging crews were called in for the lift of the tank lids and crucible swaps. While the lids were removed, new C-ring seals were installed on the tanks. A new annular ring-type lid (shown in Figure 20) was also fabricated to enable installation of the bearing test rig.

Figure 20. Lift and swap of existing Nickel 201 crucibles with new UNS S31600 variants. A new annular ring-type lid (right) was also fabricated to enable installation of the bearing test rig.

Task 3.6: Assembly of major supporting components

Assembly of major supporting components was a satisfying phase of the project because significant progress was realized through the installation of the following (as shown in Figure 21–Figure 23):

- Base plate heaters
- A spring-loaded base to enable thermal expansion of the bearing test rig
- Lifting operations to position the tanks
- Heating jackets for axial temperature zone control
- Insulating jackets to minimize heat loss

Figure 21. Installation of base plate heaters, tanks, and pump stand.

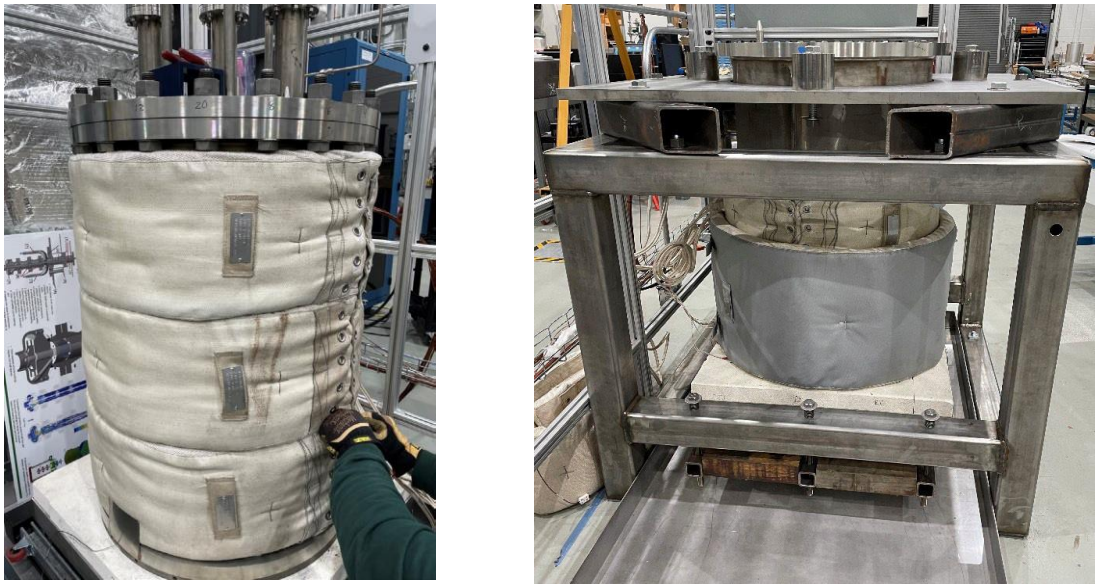

Figure 22. Installation of heating and insulating jackets.

Figure 23. Awaiting delivery of the bearing test rig.

Task 3.7: Integrate the bearing test rig

Integration of the bearing test rig with the facility involved shipping, receiving, unpacking, inspecting, lifting, and sealing operations (as shown in Figure 24–Figure 26).

Figure 24. Shipping and receiving of the bearing test rig.

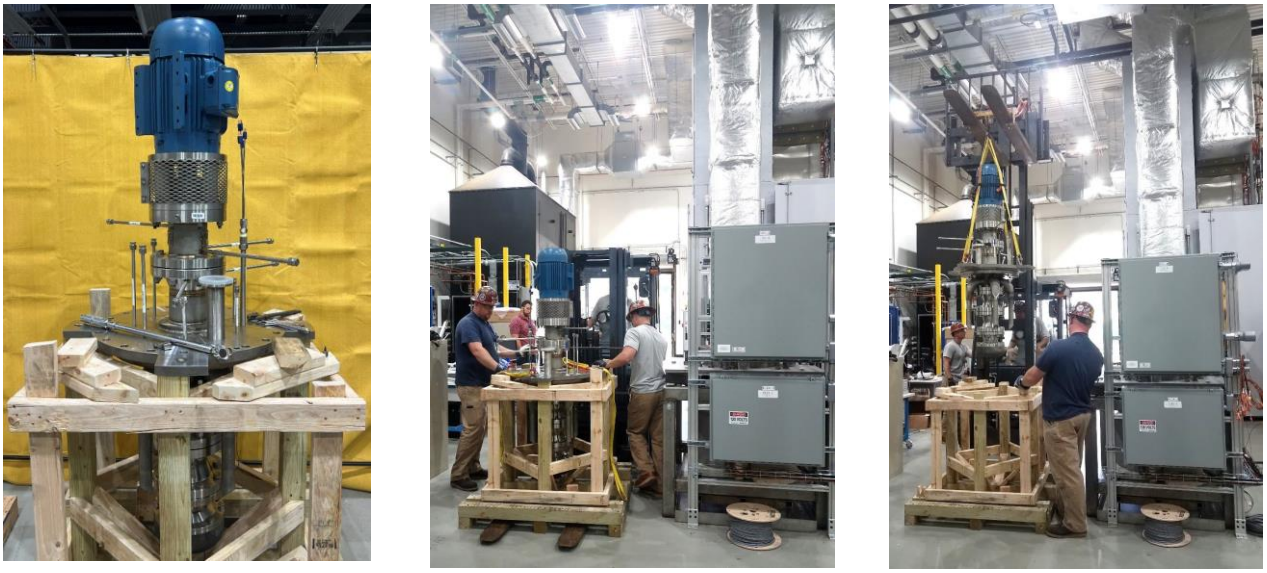

Figure 25. Installation of the bearing test rig.

Figure 26. Completion of bearing test rig integration.

Task 3.8: Salt purification

Task 3.8.1: Procure

Approximately 200 kg of anhydrous carnallite salt was received from Israel Chemicals Ltd. Sufficient quantities of the Silver Peak halite salt from Albemarle Inc. are also on hand. The combination of these two products yields the desired ternary Gen 3 CSP $MgCl_2$-KCl-NaCl salt. These are the same salt products used for the FASTR facility [2].

Figure 27. Anhydrous carnallite salt (200 kg) from Israel Chemicals Ltd.

Task 3.8.2: Salt transfer system

The existing purification system for FASTR [2] was intended to be used for purification. The system is housed within a ventilated enclosure adjacent to the pump bearing test rig. Salt transfer tubing was designed and procured to transfer salt from the purification vessel to the test setup.

Task 3.8.3: Purify salt

Salt purification was scheduled to be the last task of the facility setup. Because of project time and budget constraints, this task was not initiated.

Task 3.9: Disassembly equipment

Consideration was made in the bearing test rig's design to aid in disassembly so that the planned disassembly and inspection tasks could be completed. Disassembly is often difficult in applications that involve high-temperature and salt-wetted components.

A cantilevered frame was constructed to support the test rig and enable 270˚ access to the volute, impeller, column assembly, shaft, spiders, and bearings. A wash tank was also procured to enable soaking of the pump in deionized water to dissolve remaining salt and ease disassembly. Existing ultrasonic equipment was identified if determined to be needed to aid salt dissolution. Hot work permits for torching activities and wash tank waste disposal procedures were investigated.

Task 3.10: Cold leaking testing

Pressurized cold leak testing of the storage tank and pump tank was completed. The storage tank held a constant pressure for 24 h, indicating that the main flange seal and access port seals were functioning properly.

A pinhole leak was identified in the bearing test rig around a fillet weld sealing a penetration for the thrust bearing active cooling. After being repaired, the tank held a constant pressure for 24 h, indicating that the main flange seal and access port seals were functioning properly.

Task 3.11: Hot leak testing

Hot leak testing was planned but not conducted prior to the end of the project.

Task 4: Bearing Testing

The bearing test plan consisted of two rounds of testing. The first test was planned for 500 h of continuous operation. The second round of testing depended on the performance during the first round of testing. The second test was to either be longer in duration or use a revised bearing design.

One round of full-scale bearing tests would be performed. The first test would run three bearings at a single speed for 500 h (21 days). After the test, the bearings would be removed and examined for wear and corrosion. The methods used for the past static corrosion capsule and tribology tests would be followed. Additionally, changes in the macroscopic dimensions of the bearing (i.e., annular gap and roundness) would be assessed. If warranted, a second test would be performed based on the results of the first test; this test would depend on performance during the first round of testing. The second test could have been a long duration run of 1,000 h (42 days), during which the shaft would be cycled on and off two times per day or a different bearing-to-shaft radial gap would be tested. After the second test, the bearings would have been removed and analyzed using the same methods as the first test. During these tests, at least three corrosion coupons of each material of interest would have been immersed in the salt

(i.e., coupons submerged in the tank and physically separate from the bearings). The corrosion and/or surface finish changes of these test coupons would then be compared to the bearings to elicit any unique tribocorrosion effects. Unfortunately, Test 1 (Task 4.1) and Test 2 (Task 4.2) were not initiated before the end of the project.

Significant Accomplishments and Conclusions

The tribological testing with added impurities was novel. This testing provided the first published insight into the effects of impurities (i.e., concentration and size distribution) on the tribological performance of candidate bearing materials in a high-temperature chloride salt environment.

First-of-a-kind journal bearings of relevant size for molten salt service were successfully designed and fabricated. A test rig for conducting demonstrations and performing tests to mitigate risks for molten salt pump technology was also designed, fabricated, and installed. The accompanying test equipment needed to conduct high-temperature halide salt testing was also designed, procured, and installed. Altogether, a new national capability to the mitigate the risks of molten salt pump technology at a relevant scale was developed.

Several challenges affected the project schedule and budget:

- Magnetic motor-shaft coupling of the 10 HP motor: The sponsor advised (based on previous experience) increasing the sizing of the motor to 10 HP. The magnetic coupling for this size motor was a nonstocked size that carried a long lead time.
- YTZP bushing fabrication: Tooling at the vendor/manufacturer for the bushing was protracted, resulting in delayed receipt.
- Metal fabrication: The flange faces were initially out of specification, causing misalignment of the assembled test rig and issues during the first water test. These faces had to be re-machined, a process that required disassembly and reassembly of the test rig.
- Additional water shakedown testing: Because of the aforementioned issue, an additional series of shakedown tests was performed.
- Improper weld: A defect in a gas space weld was identified during pressurized cold leak testing. This defect was addressed.

These challenges are primarily related to fabrication and the industrial supply chain rather than the technical feasibility of the candidate bearings. Unfortunately, these challenges, which affected the project schedule and budget, resulted in the bearings not being tested.

Inventions, Patents, Publications, and Other Results

A journal paper was published on the tribological effects of particles in molten chloride salt: He, Xin, et al. "Effects of Particle Size and Concentration of Magnesium Oxide on the Lubricating Performance of a Chloride Molten Salt for Concentrating Solar Power." *ACS Sustainable Chemistry & Engineering* 9.14 (2021): 4941–4947.

A story highlight on the pump bearing test stand was published on ORNL's public website: *https://www.ornl.gov/organization-news/ornl-sets-molten-salt-test-stand-thermal-hydraulics-laboratory*
The project also facilitated ongoing collaboration between the national laboratories, advanced materials manufacturers, and molten salt pump manufacturers.

Path Forward

Because the molten salt bearing test stand has been constructed and is ready for testing, ORNL has continued to reach out to potential stakeholders within the pump community to explore potential testing and risk mitigation needs to support commercialization of this promising technology.

Recently, there have been additional studies related to molten salt tribology:

- NiWC-based salt-wetted bearings were successfully tested at 720°C in the ternary chloride salt of interest for 500 h [14].
- Additional pin-on-disc tribology tests have been conducted in a fluoride salt (LiF-NaF-KF eutectic) with several material parings at temperatures ranging from 550°C to 650°C [15, 16, 17].
- An additional study investigated MgO particles in the ternary salt of interest after purification at the 3 kg scale. From the top and middle sampling locations of the purified salt, the mean particle size was approximately 40 µm based on volume weighting and 2.6 µm based on number weighting, and there was a total of <0.03 wt % of insoluble species [18]. These results generally corroborate the earlier findings from Zhou [12].

Several areas for further investigation were identified during the project:
Fundamental studies:

- **Effect of particulate in the salt on bearing performance and life**: Pin-on-disc tests showed that the particulate can have a deleterious effect on bearing wear and friction. However, the pin-on-disc tests also showed a complicated relationship between phenomena (e.g., adhesion, 3-body wear, increased hardness) and the materials tested. An expanded test matrix would provide additional insight into the phenomena and guide future material selection.
- **Particulate evolution (quantity and size) in the salt**: Two existing studies of postpurified salt provide some insight into the particulate size that may be encountered. However, these studies were performed on samples taken from relatively small batches of salt purified under laboratory-controlled conditions. The evolution of particulate characteristics in an "aged" industrial system remains unknown.

Applied studies:

- Demonstrate bearing life under prototypical conditions.
- Understand the effects of particulate, temperature, and start/stop cycles on bearing performance and life.
- Demonstrate recovery from frozen salt in bearing.
- Study performance of bearings located in the gas space above molten salt.
- Demonstrate bearing replacement.

References

1. Mehos, Mark, et al. 2017. “Concentrating Solar Power Gen3 Demonstration Roadmap.” NREL/TP-5500-67464. National Renewable Energy Laboratory.
2. Robb, K. R., S. Baird, J. Massengale, N. Hoyt, J. Guo, and C. Moore. 2022. “Engineering-Scale Batch Purification of Ternary $MgCl_2$-KCl-NaCl Salt Using Thermal and Magnesium Contact Treatment.” 2022. ORNL/TM-2022/2554. Oak Ridge National Laboratory.
3. Robb, K. R., S. Baird, J. Massengale, E. Kappes, and P. Mulligan. 2022. “Facility to Alleviate Salt Technology Risks (FASTR): Design Report.” ORNL/TM-2022/2803. Oak Ridge National Laboratory.
4. Robb, K. R., and Ethan Kappes. 2023. “Facility to Alleviate Salt Technology Risks (FASTR): Commissioning Update.” ORNL/TM-2023/2846. Oak Ridge National Laboratory.
5. Turchi, Craig S., et al. 2021. “CSP Gen3: Liquid-Phase Pathway to SunShot.” NREL/TP-5700-79323. National Renewable Energy Lab.
6. Robb, K. R., Prashant K. Jain, and Thomas J. Hazelwood. "High-Temperature Salt Pump Review and Guidelines—Phase I Report." 2016. ORNL/TM- 2016/199. Oak Ridge National Laboratory.
7. Barth, D. L., J. E. Pacheco, W. J. Kolb, and E. E. Rush. 2002. "Development of a High-Temperature, Long-Shafted, Molten-Salt Pump for Power Tower Applications." *J. Sol. Energy Eng.* 124(2): 170–175. https://doi.org/10.1115/1.1464126.
8. Oldinski, Keith. 2021. “Development of High Temperature (> 700° C) Molten Salt Pump Technology for Gen3 Solar Power Tower Systems.” DOE-HTI-0008373-1. Hayward Tyler, Inc.
9. Keiser, James R., et al. 2023. "Material Selection and Corrosion Studies of Candidate Bearing Materials for Use in Molten Chloride Salt." *J. Sol. Energy Eng.* 145(2): 021001.
10. He, Xin, et al. "Tribological behavior of ceramic-alloy bearing contacts in molten salt lubrication for concentrating solar power." 2021. *Solar Energy Materials and Solar Cells* 225: 111065.
11. He, Xin, et al. 2021. "Effects of Particle Size and Concentration of Magnesium Oxide on the Lubricating Performance of a Chloride Molten Salt for Concentrating Solar Power." *ACS Sustainable Chemistry & Engineering* 9(14): 4941–4947.
12. Zhao, Youyang. 2020. “Molten Chloride Thermophysical Properties, Chemical Optimization, and Purification.” NREL/TP-5500-78047. National Renewable Energy Laboratory.
13. Raiman, Stephen S., et al. 2019. “Compatibility studies of cladding candidates and advanced low-Cr superalloys in molten NaCl-MgCl2.” ORNL/TM-2019/1132. Oak Ridge National Laboratory.
14. Ogren, Evan, et al. 2023. "Tribology of high toughness NiWC components in molten ternary chloride salt." *AIP Conference Proceedings* 2815(1). AIP Publishing.

15. He, Xin, et al. 2023. "Tribocorrosion of stainless steel sliding against graphite in FLiNaK molten salt." *Wear* 522: 204706.
16. Ma, Jiqiang, et al. 2023. "High temperature tribological properties of the D-gun WC-12Co coating in fluoride molten salt." *Wear* 530: 205031.
17. Xiao, Rongzhen, et al. 2023. "High temperature tribological properties of D-gun Al2O3 coatings in fluoride molten salts." *Surface and Coatings Technology* 458: 129350.
18. Guo, Jicheng, et al. 2023. “Continuous Particle Monitoring and Removal for Molten Chloride CSP Systems.” ANL/CFCT-23/1. Argonne National Laboratory.